



**HAL**  
open science

## Determining the change in length of the anterolateral ligament during knee motion: A three-dimensional optoelectronic analysis

Thomas Neri, Rodolphe Testa, Loic Laurendon, Margaux Dehon, Sven Putnis, Samuel Grasso, David Parker, Frédéric Farizon, Rémi Philippot

### ► To cite this version:

Thomas Neri, Rodolphe Testa, Loic Laurendon, Margaux Dehon, Sven Putnis, et al.. Determining the change in length of the anterolateral ligament during knee motion: A three-dimensional optoelectronic analysis. *Clinical Biomechanics*, 2019, 62, pp.86-92. 10.1016/j.clinbiomech.2019.01.006 . hal-02464951

**HAL Id: hal-02464951**

**<https://univ-lyon1.hal.science/hal-02464951>**

Submitted on 21 Oct 2021

**HAL** is a multi-disciplinary open access archive for the deposit and dissemination of scientific research documents, whether they are published or not. The documents may come from teaching and research institutions in France or abroad, or from public or private research centers.

L'archive ouverte pluridisciplinaire **HAL**, est destinée au dépôt et à la diffusion de documents scientifiques de niveau recherche, publiés ou non, émanant des établissements d'enseignement et de recherche français ou étrangers, des laboratoires publics ou privés.



Distributed under a Creative Commons Attribution - NonCommercial 4.0 International License

1 **Determining the Change in Length of the Anterolateral Ligament During Knee Motion:**  
2 **A Three-Dimensional Optoelectronic Analysis.**

3  
4 Thomas Neri, MD, PhD<sup>1,2,3\*</sup>

5 Rodolphe Testa, PhD<sup>1</sup>

6 Loic Laurendon, MD<sup>2</sup>

7 Margaux Dehon<sup>2</sup>

8 Sven Putnis, MD<sup>3</sup>

9 Samuel Grasso, PhD<sup>3</sup>

10 David A Parker, MD<sup>3</sup>

11 Frederic Farizon MD<sup>1,2</sup>

12 Remi Philippot, MD, PhD<sup>1,2</sup>

13  
14 <sup>1</sup> Univ Lyon – UJM-Saint-Etienne, Inter-university Laboratory of Human Movement Science,  
15 EA 7424, F-42023, Saint-Etienne, France

16  
17 <sup>2</sup> Department of Orthopedic Surgery, University Hospital of Saint Etienne, France

18  
19 <sup>3</sup> Sydney Orthopaedic Research Institute, Sydney, Australia

20 \*corresponding author: [thomas.neri@chu-st-etienne.fr](mailto:thomas.neri@chu-st-etienne.fr), Inter-university Laboratory of Human  
21 Movement Science, CAMPUS SANTE INNOVATIONS Bâtiment IRMIS, 10 rue de la  
22 Marandière, 42270 Saint Priest en Jarez, +33477421875

23  
24  
25 **COMPLIANCE WITH ETHICAL STANDARDS**

26 Conflict of Interest: The authors declare that they have no conflict of interest.

27 Funding: This research did not receive any specific grant from funding agencies in the public,  
28 commercial, or not-for-profit sectors.

29 Ethical approval: This article does not contain any studies with human participants or animals  
30 performed by any of the authors.

31  
32  
33 **ABSTRACT:** 234 words

34 **MANUSCRIPT:** 2596 words

35

36

37 **ABSTRACT**

38

39 *Background:* The variation of the anterolateral ligament (ALL) length during knee motion is  
40 still unclear, and the knee position in which a reconstruction graft should be tensioned  
41 remains controversial. The objective of this study was to determine the variation of the ALL  
42 length during knee motion using a three-dimensional optoelectronic system.

43 *Methods:* Kinematic analyses of 20 cadaveric knees were performed using a Motion  
44 Analysis® system. The variability of the measurements made during the five acquisition  
45 cycles was studied. Reliability was evaluated by two separate measurement sessions, with  
46 complete system reinstallation, using different cadavers and a new operator. The ALL length  
47 was analysed from extension to full flexion in three rotational conditions.

48 *Findings:* When analysing the reliability of the five cycles, 82% of the measurements we  
49 found to have an Intra Class Correlation (ICC) >0.85. The reproducibility of inter-sessional  
50 measures by different operators and different cadavers was either good (ICC >0.75) or  
51 excellent (ICC >0.85). The ALL length was maximum in full internal rotation with the knee  
52 at 25° of flexion.

53 *Interpretation:* This three-dimensional optoelectronic protocol allowed us to analyse the  
54 variation of the ALL length during intact knee motion with good reliability and the required  
55 accuracy to analyse this variable. The maximal length and highest tension of the ALL was  
56 reported at 25° of knee flexion in internal rotation, suggesting this as the optimal position for  
57 the knee joint when tensioning an ALL reconstruction.

58

59 **KEYWORDS:** knee, Anterolateral ligament, kinematic, length, optoelectronic system

60

## 61 INTRODUCTION

62  
63 Good control of rotational stability after intra-articular anterior cruciate ligament (ACL)  
64 reconstruction is not always achieved and there has been a renewed interest in the role of  
65 extra-articular structures, among them the anterolateral ligament (ALL) (Claes et al., 2013;  
66 Neri et al., 2018a). Combined ACL and ALL reconstructions in ACL deficient knee have  
67 been suggested to offer clinical and biomechanical advantages in controlling anterolateral  
68 rotational laxity more than an isolated ACL reconstruction in ACL-deficient knee (Geeslin et  
69 al., 2018b; Sonnery-Cottet et al., 2015). During ALL reconstruction it is necessary to fix the  
70 graft in a position close to its maximum length, corresponding to its range of action, in order  
71 to restore normal biomechanics, and avoid insufficient tension or overconstraint. To date there  
72 is no consensus on this point and different surgical techniques have subsequently appeared,  
73 fixing the graft either with the knee in full extension (Sonnery-Cottet et al., 2015), at 30° of  
74 flexion (Chahla et al., 2016), or at 90° of flexion (Helito et al., 2015). A detailed  
75 understanding of the biomechanical behaviour of the ALL is therefore required to facilitate an  
76 optimal reconstruction technique.

77  
78 The first studies undertaken to evaluate the variation of the ALL length were static analyses  
79 using digital calipers measurements at predetermined flexion and rotational values (Claes et  
80 al., 2013; Neri et al., 2017; Runer et al., 2016). Three-dimensional imaging analyses have also  
81 been used (Helito et al., 2014; Kernkamp et al., 2016; Van de Velde et al., 2016; Wieser et al.,  
82 2017). Although having the advantage to be performed on in vivo subjects, these models were  
83 created from theoretical insertions points, which are difficult to identify on MRI and subject  
84 to significant inter-individual variability (Daggett et al., 2016; Neri et al., 2018b; Parker and  
85 Smith, 2016). Other studies used freedom robotic systems or knee rig systems (Dodds et al.,  
86 2014; Drews et al., 2017; Geeslin et al., 2018a; Kittl et al., 2015; Parsons et al., 2015). These  
87 systems have excellent reliability and optimal precision by dispensing with manipulation by a  
88 human operator. Yet all these studies used isolated knees, with sectioning of the musculo-  
89 tendinous structures around the knee, such as the biceps femoris tendon and Iliotibial Band  
90 (ITB) subsequently losing their contribution to the rotational stability of the knee and  
91 potentially affecting the ALL function (LaPrade et al., 2005; Rahnemai-Azar et al., 2016).  
92 Surgical navigation systems designed for prosthetic knee surgery have also been used with the  
93 advantage of conserving the full leg and the ITB (Bonanzinga et al., 2016; Imbert et al.,  
94 2016). However, these studies assessed the ALL length without combining both continuous  
95 flexion and rotation kinematics. Internal rotation was applied only for some target flexion  
96 values (20 and 90° for Imbert, and 30 and 90° for Bonanzinga). In addition, these systems use  
97 few cameras with lower data acquisition frequencies, making it difficult to assess the  
98 biomechanical behaviour of the ALL (Güler et al., 2013).

99  
100 Consequently, there are contradictions in current biomechanical results when describing the  
101 variation in ALL length during motion leading to inconsistencies about the position of the knee  
102 at which the ALL is at maximum length. We hypothesised that the use of another  
103 measurement device, a three-dimensional optoelectronic system, such as the Motion  
104 analysis®, would allow the assessment of combined continuous flexion and rotation  
105 kinematics and lead to an accurate and reliable measurement of the ALL length. The objective  
106 of this study was therefore to determine the variation of the ALL length during knee motion.

108 **METHODS**

109

110 **1. Specimen preparation**

111 Twenty-two intact knees from 11 fresh frozen cadaveric specimens were used. The specimens  
112 were thawed out at room temperature for 24 hours and showed no signs of degeneration.  
113 Exclusion criteria were examination signs of knee instability (anterior tibial drawer and  
114 positive pivot-shift test), evidence of prior knee surgery or ACL reconstruction, severe  
115 deformities or severe knee osteoarthritis. An anteromedial knee arthroscopy was performed to  
116 confirm the Anterior Cruciate Ligament (ACL) status. A total of two knees were subsequently  
117 excluded and 20 intact knees without ACL and ALL injuries were included. There were 5  
118 men and 5 women with a mean age of 68.9 years (range, 57 to 85).

119 We used the full leg and pelvis in order to preserve the entire length of the ITB and all other  
120 synergistic bi-articular structures crossing the hip and/or the knee. The dissection protocol  
121 used to define the ALL was described in a previous anatomical study (Neri et al., 2017). The  
122 number of incisions was kept to the strict minimum in order to limit their effects, and they  
123 were always made in line with the tendinous fibres. No lateral structures were removed. The  
124 femoral origin of the ALL was always posterior and proximal to the lateral femoral  
125 epicondyle and its tibial insertion was posterior to Gerdy's tubercle, anterior to the fibular  
126 head and distal to the articular cartilage of the lateral tibial plateau. At the end of the  
127 dissection, once the insertions were recorded and the acquisitions made, the ITB was  
128 anatomically closed.

129

130 **2. Experimental set-up**

131 Superior acetabular screws fixed the pelvis to the table and the cadavers were positioned to  
132 allow free range of motion of the knee over the edge of the table (Figures 1B and 1C).

133 Kinematic analysis was performed using a Motion Analysis® (Motion Analysis corp., Santa  
134 Rosa, CA, USA) stereophotogrammetry system. The system consisted of 8 high-definition  
135 Raptor-E® cameras operating at 100 Hz (Figure 1A). After installation and calibration around  
136 the working area the system followed retro-reflective sensors (Targets). A pelvic marker was  
137 defined from 3 targets fixed on the ipsilateral anterior superior iliac spine. The femur and the  
138 tibia were equipped with 4 targets each: F1 to F4 and T1 to T4 (Figure 2). These targets were  
139 fixed using bi-cortical pins placed in such a way as to leave free the muscles and ligaments.  
140 Three points are sufficient to reconstruct the movements of a solid in space, and the use of the  
141 fourth provided a backup in the event of disengagement of a target or temporary masking.  
142 Using a navigation probe, points of interest were next identified. The epicondyles and  
143 malleoli were then calculated (Figure 2, purple stars) from these palpated points (Figure 2,  
144 purple circles). The centre of the hip was calculated kinematically via circumduction (Gamage  
145 and Lasenby, 2002) to overcome the hip movement during knee motion (Figure 2, purple  
146 star). The centre of Inter Condylar Eminences (ICE) was located arthroscopically. The set of  
147 points determines the axes and the femoral and tibial references as defined in ISB conventions  
148 and the work of Grood and Suntay (Grood and Suntay, 1983; Wu et al., 2002). The centre of  
149 the tibial and femoral insertion points of the ALL were identified by internally rotating the  
150 tibia and determining the course of the central ligamentous fibres coming under the most  
151 tension; the position for the optimal surgical reconstruction.

152

153 **3. Determining the Change in Length of the ALL**

154 The study was divided into two separate sessions of 10 knees each, separated by one month  
155 and performed by two different operators in order to appreciate the reliability of the  
156 experimental process. The knees were different between the two sessions.

157 We studied the knee flexion kinematics in three different test conditions: Forced internal  
158 rotation (IR) Forced external rotation (ER) and neutral rotation (NR. For NR, the foot was  
159 placed in neutral rotation and the tibia in its reduced position with respect to the femur with  
160 unconstrained tibial rotation. A dynamometric torque rig triggering at 5nm, placed above the  
161 ankle at the axis of rotation joint and fixed by 2 pins, provided rotation (Figure 3).  
162 The knee was flexed manually by moving the tibia relative to the femur from complete  
163 extension to 90° of flexion while controlling the rotation with the dynamometric torque rig. In  
164 every test condition, this movement was repeated five times and performed with a very slow  
165 speed of 5 seconds per movement corresponding to an average speed of  $\pi / 10 = 0.3 \text{ Rad.s}^{-1}$ .  
166 After processing the kinematics using Cortex® software, the data was filtered (Butterworth  
167 filter of order 4 with a cut off frequency of 6 Hz) according to Winter and Pezzack (Pezzack  
168 et al., 1977; Winter et al., 1974). The recorded data was interpolated to obtain values from full  
169 extension to 90° of flexion at each degree of flexion. Therefore, we could determine the  
170 internal-external rotation angle (ROT) and the distance between the femoral and tibial  
171 insertions of the ALL (ALL length) during the full range of knee motion (Figure 4).

172

#### 173 **4. Statistical analysis**

174 All statistical analyses were performed using SPSS® software (IBM, Armonk, New York,  
175 United States).

176 Initial statistical analysis was for reliability of the five cycles during the kinematic  
177 acquisitions for the three conditions of rotation (IR, ER and NR) and for both variables of  
178 interest (ROT, ALLlength). This analysis included all the knees (n=20 knees). A statistical  
179 test of the intraclass correlation coefficient (ICC) was used for each measured variable (ROT,  
180 ALLlength). According to Smith-Crowe et al., ICC was considered good if it was  $\geq 0.75$  and  
181 excellent if it was  $\geq 0.85$  (Smith-Crowe et al., 2013). For accepting data without modification,  
182 a threshold of 0.85 was required. Two-way mixed ICC calculations with an absolute  
183 agreement search were performed. A second statistical analysis was performed to evaluate the  
184 reliability of our protocol between the two separate measurement sessions (for each session,  
185 n=10 knees). Using the statistical method described above, we calculated the mean curves of  
186 the measurements (ROT, ALLlength) during the two sessions for the three test conditions (IR,  
187 ER and NR). The ICC of these average curves was then calculated from the data from these  
188 two sessions (two-way randomized ICC). In order to compare the lengths of ALL between the  
189 IR, NR and ER, a variance analysis study (ANOVA) was performed on repeated  
190 measurements. P values less than 0.05 were considered statistically significant.

191

192

193 **RESULTS**

194

195 **Accuracy and Reliability**

196 The average error of target positioning was consistently less than 0.15 mm and the  
197 measurement error of the angles was less than 0.2 degrees.

198 In the first analysis on the reliability of the five cycles, ICCs were performed for 120  
199 measurements. 82% of these values had an ICC > 0.85 and did not require curve suppression.  
200 15% required the removal of one curve to obtain an ICC  $\geq$  0.85. 3% required the removal of 2  
201 curves. In one case, the worst, the ICC after removal of 2 curves was 0.76. Figure 5 illustrates  
202 the variability of the measurements (acquisitions) for a knee.

203 The second analysis showed either good or excellent reproducibility between the two sessions  
204 with different operators and different knees. For the ROT measurement, the ICC was 0.93 in  
205 IR and 0.83 in ER. For the ALL length measurement, the ICCs were 0.86 in IR, 0.99 in ER,  
206 and 0.98 in NR.

207

208 **Determining the Change in Length of the ALL**

209 After determination of the femoral and tibial insertion points of the ALL, it was then possible  
210 to measure the length of the ALL throughout the full range of motion. This length was studied  
211 for the 3 rotational conditions in order to determine the flexion and rotation conditions for  
212 which the ALL was overtight (maximum length). There was a significant difference for ALL  
213 length between the IR and the NR rotation ( $p < 0.001$ ), whatever the knee flexion (Figure 6). In  
214 contrast, there was no significant difference between NR and ER ( $p > 0.05$ ). The ALL length  
215 was maximum in IR at 25 ° of knee flexion. It should be noted that there is considerable  
216 variation in ALL length between individual knee specimens, which is indicated in figure 6 as  
217 the extended error bars for the ALL length at different degrees of knee flexion.  
218

219 **DISCUSSION**

220

221 By using an accurate and reliable three-dimensional optoelectronic system, we were able to  
222 analyse the variation in length of the ALL during motion in an intact knee. We demonstrated  
223 that its maximum length was in IR at 25° of knee flexion.

224

225 Compared to other experimental tools, such as robotic, 3D scan model and traditional  
226 navigation systems, our protocol was the first to use a stereophotogrammetry system such as  
227 Motion analysis®, recognized as the current gold standard for an instrument evaluating  
228 kinematics in three-dimensions. This measurement tool allowed us to obtain continuous knee  
229 kinematics combining flexion and rotation in a full lower limb with all the bi-articular  
230 structures conserved. By determining the change in length of the ALL during knee motion,  
231 the aim of this study has been fulfilled with the required accuracy to analyse the small change  
232 in this variable and with good reproducibility of the kinematic assessments.

233 Experimental accuracy depends on the type of sensor fixation used, the number and  
234 configuration of the cameras used and the size of the work volume. To reduce the incidence of  
235 experimental errors, we used a large number of cameras (8 HD cameras), a volume restricted  
236 to the maximum (0.8 m / 1.2 m / 1.5 m), stable bone fixation, and a wide inter-distance  
237 between two targets. The mean error was always less than 0.15 mm and the angle  
238 measurement error was less than 0.2 degrees. This protocol therefore has optimal precision for  
239 acquisition of data and far greater than when determining the centre of the anatomical  
240 insertions; the ALL insertion points cover areas over 5 mm<sup>2</sup> and it is difficult to precisely  
241 evaluate the centre. In order to minimize this bias, all dissections were made by an  
242 experienced operator who observed the position of the ALL during internal tibial rotation.

243 Regarding the reproducibility, this protocol demonstrated a good intra-rater reliability  
244 between measurements with 82% of ICCs superior to 0.85. In addition, this protocol  
245 demonstrated either good or excellent inter-sessional reliability when compared with a second  
246 session with new cadaveric set-ups and operator. This makes it possible to validate its use in  
247 multisession biomechanical studies.

248

249 The protocol described in this study will have many clinical applications. In vitro, it will  
250 allow the in-depth study of healthy knee kinematics, or after injury of the ACL and  
251 anterolateral complex (ALC). The individual functions of structures composing the ALC  
252 (ALL, anterolateral capsule, and iliotibial band Kaplan fibres) are still controversial and  
253 unclear. Their individual contribution to the anterolateral rotational laxity require an accurate  
254 experimental assessment. It can also be applied to the post-operative knee providing a greater  
255 understanding of the role of the ALL reconstruction in providing additional rotational control,  
256 and how it may alter knee kinematics.

257 In vivo, this study provides a useful information to guide ALL reconstruction that may be  
258 required in primary surgery for patients with a combined ACL and ALC injury as well as  
259 those requiring revision surgery after a first failed ACL reconstruction (Sonnery-Cottet et al.,  
260 2017, 2015). Although this additional procedure has shown clinical and biomechanical  
261 benefits (Geeslin et al., 2018b; Sonnery-Cottet et al., 2015), there are still inconsistencies in  
262 graft fixation. In order to ensure efficient and physiological biomechanical behaviour, the  
263 graft has to be fixed close to the range of flexion where the ALL operates, i.e when it is  
264 tensioned. To date, there is no clear consensus on this point. Regardless of measurement and  
265 instrumentation factors, the literature suggests that the other main factor influencing the  
266 length is the location of the ALL femoral origin (Monaco et al., 2017). Helito *et al.*,  
267 recommends that the graft is fixed with the knee flexed between 60 and 90° (Helito et al.,  
268 2015, 2013) with the ALL femoral footprint identified either anterior or on the lateral femoral

269 epicondyle. Sonnery-Cottet *et al.*, recommend graft fixation close to extension and neutral  
270 rotation to avoid overtightening in external rotation (Sonnery-Cottet et al., 2015). They  
271 located the ALL femoral origin posterior to the epicondyle. In another study, the same team  
272 demonstrated that the ALL is tight when the knee is at 20° of flexion with internal rotation of  
273 the tibia (Imbert et al., 2016). This is similar to Chahla *et al.* who recommend graft fixation at  
274 30° of flexion (Chahla et al., 2016). We also found the ALL femoral origin to be in a posterior  
275 and proximal position (Neri et al., 2017), and proved it is at its longest with the knee at 25° of  
276 flexion, suggesting that this is the most appropriate position to have the knee in when  
277 tensioning a reconstruction.

278  
279 Several limitations should be noted. Firstly, the small sample size and the variations between  
280 the individual knees and specimens has contributed to the large range in ALL length seen.  
281 With 20 knees studied, our sample size is however larger than the majority of ALL  
282 biomechanical studies with an average of 10 knees. Secondly, we did not use a rig to bend the  
283 knee with the knee range of motion performed manually. Nonetheless, the intra-rater  
284 reliability was good to excellent and the movement was performed with a low speed. This  
285 slow motion allowed to overcome the effects of speed and therefore recalculation of the  
286 angles and positions in a static model by interpolating them at each degree of flexion without  
287 using angular velocities.

## 291 **CONCLUSION**

292  
293  
294 This three-dimensional optoelectronic protocol allowed us to analyse the variation of the ALL  
295 length during knee motion with good reliability and the required accuracy to analyse this  
296 variable. This makes it a valuable protocol that can be used when carrying out future  
297 biomechanical analyses necessary to optimise ALL reconstruction techniques. The maximal  
298 length and highest tension of the ALL was reported at 25° of knee flexion in internal rotation,  
299 suggesting this as the optimal position for the knee joint when tensioning an ALL  
300 reconstruction.

304 **REFERENCES**

- 305
- 306 Bonanzinga, T., Signorelli, C., Grassi, A., Lopomo, N., Bragonzoni, L., Zaffagnini, S.,  
307 Marcacci, M., 2016. Kinematics of ACL and anterolateral ligament. Part I:  
308 Combined lesion. *Knee Surg. Sports Traumatol. Arthrosc. Off. J. ESSKA*.  
309 <https://doi.org/10.1007/s00167-016-4259-y>
- 310 Chahla, J., Menge, T.J., Mitchell, J.J., Dean, C.S., LaPrade, R.F., 2016. Anterolateral Ligament  
311 Reconstruction Technique: An Anatomic-Based Approach. *Arthrosc. Tech.* 5,  
312 e453-457. <https://doi.org/10.1016/j.eats.2016.01.032>
- 313 Claes, S., Vereecke, E., Maes, M., Victor, J., Verdonk, P., Bellemans, J., 2013. Anatomy of the  
314 anterolateral ligament of the knee. *J. Anat.* 223, 321–328.  
315 <https://doi.org/10.1111/joa.12087>
- 316 Daggett, M., Ockuly, A.C., Cullen, M., Busch, K., Lutz, C., Imbert, P., Sonnery-Cottet, B.,  
317 2016. Femoral Origin of the Anterolateral Ligament: An Anatomic Analysis.  
318 *Arthrosc. J. Arthrosc. Relat. Surg. Off. Publ. Arthrosc. Assoc. N. Am. Int. Arthrosc.*  
319 *Assoc.* 32, 835–841. <https://doi.org/10.1016/j.arthro.2015.10.006>
- 320 Dodds, A.L., Halewood, C., Gupte, C.M., Williams, A., Amis, A.A., 2014. The anterolateral  
321 ligament: Anatomy, length changes and association with the Segond fracture.  
322 *Bone Jt. J.* 96-B, 325–331. <https://doi.org/10.1302/0301-620X.96B3.33033>
- 323 Drews, B.H., Kessler, O., Franz, W., Dürselen, L., Freutel, M., 2017. Function and strain of  
324 the anterolateral ligament part I: biomechanical analysis. *Knee Surg. Sports*  
325 *Traumatol. Arthrosc. Off. J. ESSKA*. <https://doi.org/10.1007/s00167-017-4472-3>
- 326 Gamage, S.S.H.U., Lasenby, J., 2002. New least squares solutions for estimating the  
327 average centre of rotation and the axis of rotation. *J. Biomech.* 35, 87–93.
- 328 Geeslin, A.G., Chahla, J., Moatshe, G., Muckenhirn, K.J., Kruckeberg, B.M., Brady, A.W.,  
329 Coggins, A., Dornan, G.J., Getgood, A.M., Godin, J.A., LaPrade, R.F., 2018a.  
330 Anterolateral Knee Extra-articular Stabilizers: A Robotic Sectioning Study of the  
331 Anterolateral Ligament and Distal Iliotibial Band Kaplan Fibers. *Am. J. Sports*  
332 *Med.* 46, 1352–1361. <https://doi.org/10.1177/0363546518759053>
- 333 Geeslin, A.G., Moatshe, G., Chahla, J., Kruckeberg, B.M., Muckenhirn, K.J., Dornan, G.J.,  
334 Coggins, A., Brady, A.W., Getgood, A.M., Godin, J.A., LaPrade, R.F., 2018b.  
335 Anterolateral Knee Extra-articular Stabilizers: A Robotic Study Comparing  
336 Anterolateral Ligament Reconstruction and Modified Lemaire Lateral Extra-  
337 articular Tenodesis. *Am. J. Sports Med.* 46, 607–616.  
338 <https://doi.org/10.1177/0363546517745268>
- 339 Grood, E.S., Suntay, W.J., 1983. A joint coordinate system for the clinical description of  
340 three-dimensional motions: application to the knee. *J. Biomech. Eng.* 105, 136–  
341 144.
- 342 Güler, Ö., Perwög, M., Kral, F., Schwarm, F., Bárdosi, Z.R., Göbel, G., Freysinger, W., 2013.  
343 Quantitative error analysis for computer assisted navigation: a feasibility study.  
344 *Med. Phys.* 40, 021910. <https://doi.org/10.1118/1.4773871>
- 345 Helito, C.P., Bonadio, M.B., Gobbi, R.G., da Mota E Albuquerque, R.F., Pécora, J.R.,  
346 Camanho, G.L., Demange, M.K., 2015. Combined Intra- and Extra-articular  
347 Reconstruction of the Anterior Cruciate Ligament: The Reconstruction of the  
348 Knee Anterolateral Ligament. *Arthrosc. Tech.* 4, e239-244.  
349 <https://doi.org/10.1016/j.eats.2015.02.006>
- 350 Helito, C.P., Demange, M.K., Bonadio, M.B., Tírico, L.E.P., Gobbi, R.G., Pécora, J.R.,  
351 Camanho, G.L., 2013. Anatomy and Histology of the Knee Anterolateral Ligament.

352 Orthop. J. Sports Med. 1, 2325967113513546.  
353 <https://doi.org/10.1177/2325967113513546>  
354 Helito, C.P., Helito, P.V.P., Costa, H.P., Bordalo-Rodrigues, M., Pecora, J.R., Camanho, G.L.,  
355 Demange, M.K., 2014. MRI evaluation of the anterolateral ligament of the knee:  
356 assessment in routine 1.5-T scans. *Skeletal Radiol.* 43, 1421–1427.  
357 <https://doi.org/10.1007/s00256-014-1966-7>  
358 Imbert, P., Lutz, C., Daggett, M., Niglis, L., Freychet, B., Dalmay, F., Sonnery-Cottet, B.,  
359 2016. Isometric Characteristics of the Anterolateral Ligament of the Knee: A  
360 Cadaveric Navigation Study. *Arthrosc. J. Arthrosc. Relat. Surg. Off. Publ. Arthrosc.*  
361 *Assoc. N. Am. Int. Arthrosc. Assoc.* 32, 2017–2024.  
362 <https://doi.org/10.1016/j.arthro.2016.02.007>  
363 Kernkamp, W.A., Van de Velde, S.K., Hosseini, A., Tsai, T.-Y., Li, J.-S., van Arkel, E.R.A., Li,  
364 G., 2016. In Vivo Anterolateral Ligament Length Change in the Healthy Knee  
365 During Functional Activities-A Combined Magnetic Resonance and Dual  
366 Fluoroscopic Imaging Analysis. *Arthrosc. J. Arthrosc. Relat. Surg. Off. Publ.*  
367 *Arthrosc. Assoc. N. Am. Int. Arthrosc. Assoc.*  
368 <https://doi.org/10.1016/j.arthro.2016.07.008>  
369 Kittl, C., Halewood, C., Stephen, J.M., Gupte, C.M., Weiler, A., Williams, A., Amis, A.A., 2015.  
370 Length change patterns in the lateral extra-articular structures of the knee and  
371 related reconstructions. *Am. J. Sports Med.* 43, 354–362.  
372 <https://doi.org/10.1177/0363546514560993>  
373 LaPrade, R.F., Bollom, T.S., Wentorf, F.A., Wills, N.J., Meister, K., 2005. Mechanical  
374 properties of the posterolateral structures of the knee. *Am. J. Sports Med.* 33,  
375 1386–1391. <https://doi.org/10.1177/0363546504274143>  
376 Monaco, E., Lanzetti, R.M., Fabbri, M., Redler, A., De Carli, A., Ferretti, A., 2017.  
377 Anterolateral ligament reconstruction with autologous grafting: A biomechanical  
378 study. *Clin. Biomech. Bristol Avon* 44, 99–103.  
379 <https://doi.org/10.1016/j.clinbiomech.2017.03.013>  
380 Neri, T., Dalcol, P., Palpacuer, F., Bergandi, F., Prades, J.M., Farizon, F., Philippot, R.,  
381 Peoc'h, M., 2018a. The anterolateral ligament is a distinct ligamentous structure:  
382 A histological explanation. *The Knee.*  
383 <https://doi.org/10.1016/j.knee.2018.03.012>  
384 Neri, T., Palpacuer, F., Testa, R., Bergandi, F., Boyer, B., Farizon, F., Philippot, R., 2017.  
385 The anterolateral ligament: Anatomic implications for its reconstruction. *The*  
386 *Knee.* <https://doi.org/10.1016/j.knee.2017.07.001>  
387 Neri, T., Parker, D.A., Beach, A., Boyer, B., Farizon, F., Philippot, R., 2018b. Anterolateral  
388 Ligament of the Knee: What we Know About its Anatomy, Histology,  
389 Biomechanical Properties and Function. *Surg. Technol. Int.* 33.  
390 Parker, M., Smith, H.F., 2016. Anatomical variation in the anterolateral ligament of the  
391 knee and a new dissection technique for embalmed cadaveric specimens. *Anat.*  
392 *Sci. Int.* <https://doi.org/10.1007/s12565-016-0386-2>  
393 Parsons, E.M., Gee, A.O., Spiekerman, C., Cavanagh, P.R., 2015. The biomechanical  
394 function of the anterolateral ligament of the knee. *Am. J. Sports Med.* 43, 669–674.  
395 <https://doi.org/10.1177/0363546514562751>  
396 Pezzack, J.C., Norman, R.W., Winter, D.A., 1977. An assessment of derivative determining  
397 techniques used for motion analysis. *J. Biomech.* 10, 377–382.  
398 Rahnama-Azar, A.A., Miller, R.M., Guenther, D., Fu, F.H., Lesniak, B.P., Musahl, V., Debski,  
399 R.E., 2016. Structural Properties of the Anterolateral Capsule and Iliotibial Band

400 of the Knee. *Am. J. Sports Med.* 44, 892–897.  
401 <https://doi.org/10.1177/0363546515623500>  
402 Runer, A., Birkmaier, S., Pamminger, M., Reider, S., Herbst, E., Künzel, K.-H., Brenner, E.,  
403 Fink, C., 2016. The anterolateral ligament of the knee: A dissection study. *The*  
404 *Knee* 23, 8–12. <https://doi.org/10.1016/j.knee.2015.09.014>  
405 Smith-Crowe, K., Burke, M.J., Kouchaki, M., Signal, S.M., 2013. Assessing Interrater  
406 Agreement via the Average Deviation Index Given a Variety of Theoretical and  
407 Methodological Problems. *Organ. Res. Methods* 16, 127–151.  
408 <https://doi.org/10.1177/1094428112465898>  
409 Sonnery-Cottet, B., Daggett, M., Fayard, J.-M., Ferretti, A., Helito, C.P., Lind, M., Monaco, E.,  
410 de Pádua, V.B.C., Thauinat, M., Wilson, A., Zaffagnini, S., Zijl, J., Claes, S., 2017.  
411 Anterolateral Ligament Expert Group consensus paper on the management of  
412 internal rotation and instability of the anterior cruciate ligament - deficient knee.  
413 *J. Orthop. Traumatol. Off. J. Ital. Soc. Orthop. Traumatol.*  
414 <https://doi.org/10.1007/s10195-017-0449-8>  
415 Sonnery-Cottet, B., Thauinat, M., Freychet, B., Pupim, B.H.B., Murphy, C.G., Claes, S., 2015.  
416 Outcome of a Combined Anterior Cruciate Ligament and Anterolateral Ligament  
417 Reconstruction Technique With a Minimum 2-Year Follow-up. *Am. J. Sports Med.*  
418 43, 1598–1605. <https://doi.org/10.1177/0363546515571571>  
419 Van de Velde, S.K., Kernkamp, W.A., Hosseini, A., LaPrade, R.F., van Arkel, E.R., Li, G.,  
420 2016. In Vivo Length Changes of the Anterolateral Ligament and Related Extra-  
421 articular Reconstructions. *Am. J. Sports Med.* 44, 2557–2562.  
422 <https://doi.org/10.1177/0363546516651431>  
423 Wieser, K., Fürnstahl, P., Carrillo, F., Fucentese, S.F., Vlachopoulos, L., 2017. Assessment  
424 of the Isometry of the Anterolateral Ligament in a 3-Dimensional Weight-Bearing  
425 Computed Tomography Simulation. *Arthrosc. J. Arthrosc. Relat. Surg. Off. Publ.*  
426 *Arthrosc. Assoc. N. Am. Int. Arthrosc. Assoc.*  
427 <https://doi.org/10.1016/j.arthro.2016.11.005>  
428 Winter, D.A., Sidwall, H.G., Hobson, D.A., 1974. Measurement and reduction of noise in  
429 kinematics of locomotion. *J. Biomech.* 7, 157–159.  
430 Wu, G., Siegler, S., Allard, P., Kirtley, C., Leardini, A., Rosenbaum, D., Whittle, M., D'Lima,  
431 D.D., Cristofolini, L., Witte, H., Schmid, O., Stokes, I., Standardization and  
432 Terminology Committee of the International Society of Biomechanics, 2002. ISB  
433 recommendation on definitions of joint coordinate system of various joints for  
434 the reporting of human joint motion--part I: ankle, hip, and spine. *International*  
435 *Society of Biomechanics. J. Biomech.* 35, 543–548.  
436  
437

438 **FIGURES**

439

440

441 **Figure 1.** Installation of Motion analysis® system with 8 High definition cameras (**1a**),  
442 around the specimen. Front (**1b**) and lateral (**1c**) pictures of the set-up showing pelvis, femoral  
443 and tibia reflective sensors.

444

445

446 **Figure 2.** Definition of bone landmarks and bone axis

447 - Femur: F1, F2, F3, F4, FHC\* (Femoral Head Center), Lateral Epicondyle (LE),  
448 Medial Epicondyle (ME), KC\* (Knee center)

449 - Tibia: T1, T2, T3, T4, center of Inter Condylar Eminences (ICE)

450 - Ankle: Medial malleolar (MM), Lateral malleolar (LM), Ankle Center\* (AC)

451 - Purple circle= palpated landmarks

452 - Purple star = calculated landmarks

453 - Femoral axis: XF (in red), YF (in green), ZF (in blue)

454 - Tibial axis: XT (in red), YT (in green), ZT (in blue)

455

456

457 **Figure 3.** Dynamometric torque rig used to control the tibial rotation applied. The rig fixation  
458 was ensured by 2 extra-articular bi malleolar (distal tibia and fibula) pins. (**3A**: draw  
459 explaining the pins positioning above the joint line of the ankle, **3B**: photograph of the rig  
460 used)

461

462

463 **Figure 4.** Example illustrating ALL length analysis during knee motion regarding rotation  
464 and flexion of the knee (ALL: anterolateral ligament)

465

466

467 **Figure 5.** Example illustrating the reproducibility of measurements over five acquisitions  
468 from one knee in three conditions (IR, NR, ER).

469 (ALL: anterolateral ligament, IR: Internal rotation, ER: External rotation, NR: Neutral  
470 rotation)

471

472

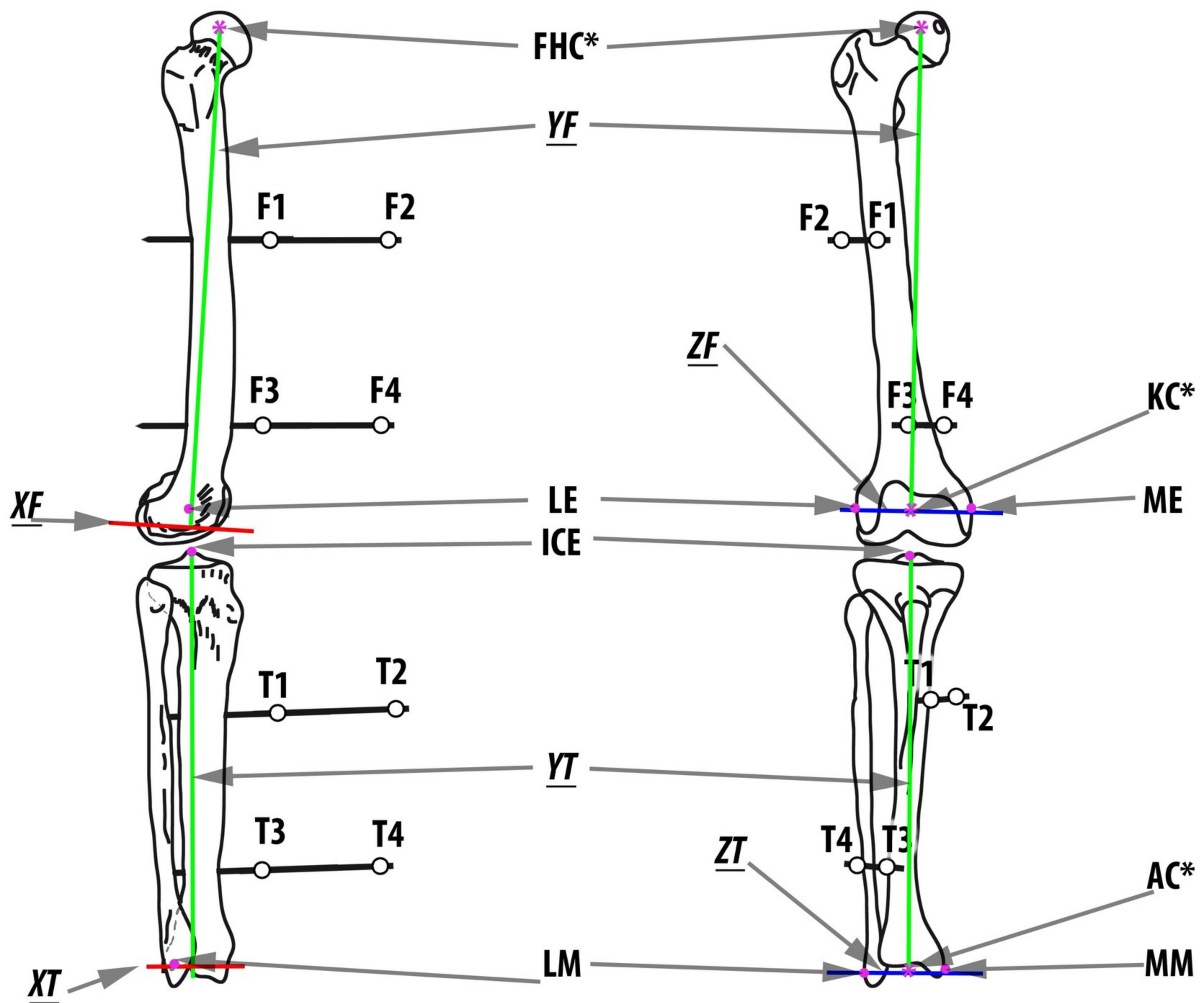
473 **Figure 6.** ALL length variation during knee flexion regarding three conditions of rotation

474 (ALL: anterolateral ligament, IR: Internal rotation, ER: External rotation, NR: Neutral  
475 rotation)

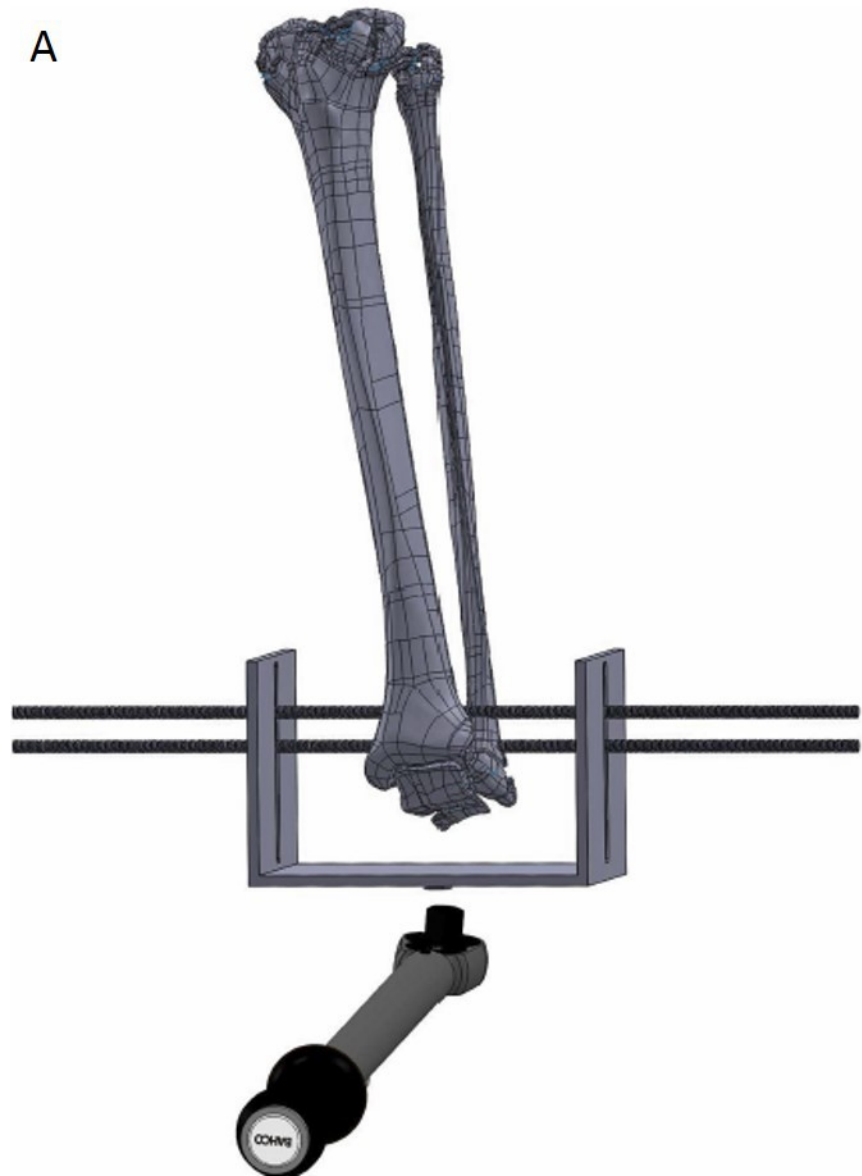
476

477

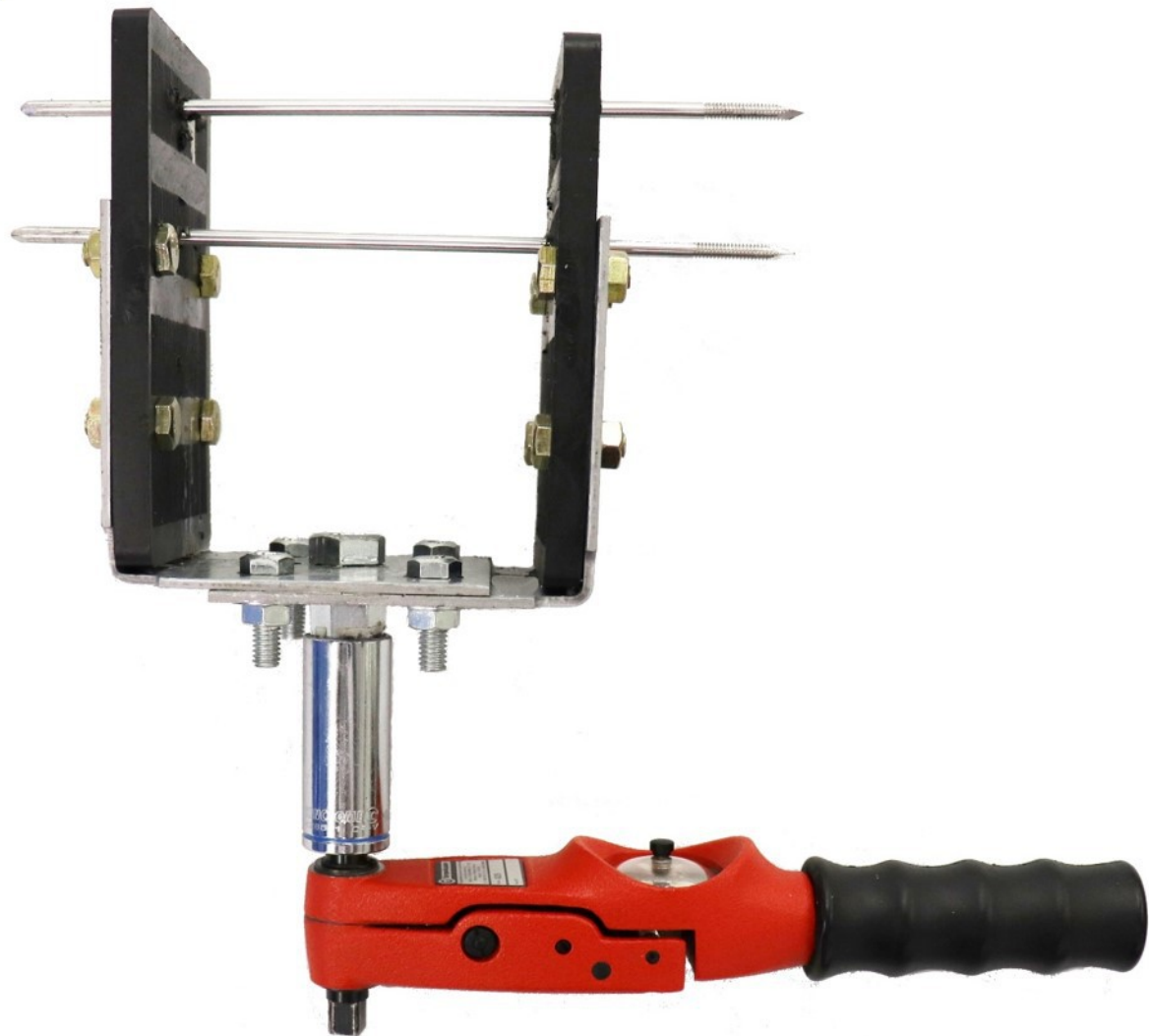


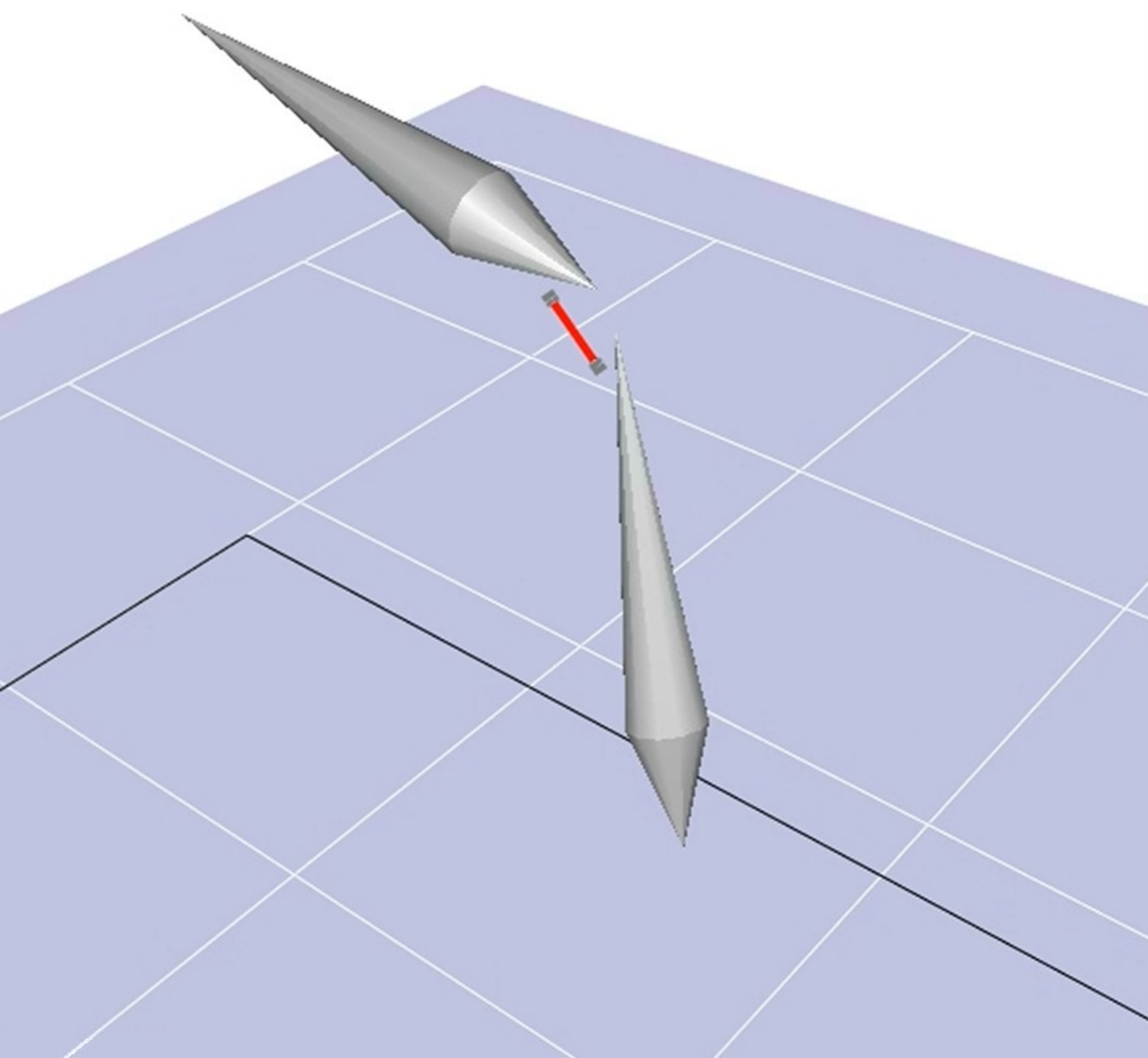


A



B

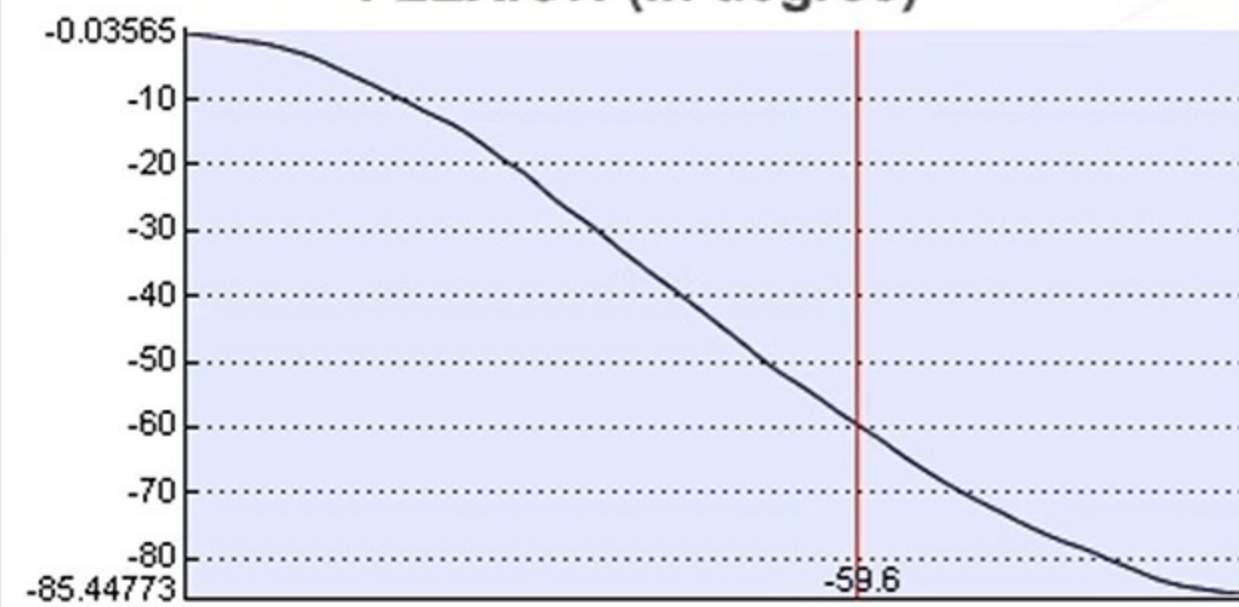




**ALL LENGTH (in mm)**



**FLEXION (in degree)**



**ROTATION (in degree)**



